nature biotechnology

LETTERS

https://doi.org/10.1038/s41587-019-0223-y

Supercooling extends preservation time of human livers

Reinier J. de Vries[1,2,3], Shannon N. Tessier[1,3], Peony D. Banik[1,3], Sonal Nagpal[1,3], Stephanie E. J. Cronin[1,3], Sinan Ozer[1,3], Ehab O. A. Hafiz[1,3,4], Thomas M. van Gulik[2], Martin L. Yarmush[1,3], James F. Markmann[1,5], Mehmet Toner[1,3], Heidi Yeh[1,5] and Korkut Uygun[1,3]*

The inability to preserve vascular organs beyond several hours contributes to the scarcity of organs for transplantation[1,2]. Standard hypothermic preservation at +4 °C (refs. [1,3]) limits liver preservation to less than 12 h. Our group previously showed that supercooled ice-free storage at −6 °C can extend viable preservation of rat livers[4,5] However, scaling supercooling preservation to human organs is intrinsically limited because of volume-dependent stochastic ice formation. Here, we describe an improved supercooling protocol that averts freezing of human livers by minimizing favorable sites of ice nucleation and homogeneous preconditioning with protective agents during machine perfusion. We show that human livers can be stored at −4 °C with supercooling followed by subnormothermic machine perfusion, effectively extending the ex vivo life of the organ by 27 h. We show that viability of livers before and after supercooling is unchanged, and that after supercooling livers can withstand the stress of simulated transplantation by ex vivo normothermic reperfusion with blood.

The absence of technology to preserve organs for more than a few hours is one of the fundamental causes of the donor organ shortage crisis[1–3]. Subzero preservation has the potential to extend the organ storage limits[1–5], as the metabolic rate halves for every 10 °C reduction in temperature[4] thereby reducing organ deterioration rate. Supercooling has the major advantage that it allows preservation at high subzero storage temperatures, while avoiding phase transitions and consequent lethal ice-mediated injury[3–5], as well as toxicity of most common cryopreservatives. However, human livers are about 200 times larger than rat livers, which exponentially increases the likelihood of heterogeneous ice nucleation during supercooling, a stochastic process that is dependent on volume and temperature[6]. Indeed, repeating the protocol we previously employed to supercool rat livers led to freezing of the livers (Supplementary Fig. 1).

We took a three-pronged approach to eliminate freezing of the livers during subzero storage. First and most critically, we minimized air–liquid interfaces, which are thermodynamically favorable sites of heterogenous ice nucleation due to surface tension. Our center (the Center for Engineering in Medicine, Harvard Medical School and Massachusetts General Hospital, Boston, MA, USA) has previously shown that by eliminating the storage medium–air interface by sealing with an immersible phase, heterogenous ice nucleation can be eliminated and up to 100 ml medium can be stored at −20 °C stably for up to 100 d (ref. [6]). While the presence of a human liver prevents the use of the same approach with the same efficacy, we minimized liquid–air interfaces by de-airing the storage solution bag ahead of supercooling to minimize such obvious ice nucleation (see Methods).

Second, we tested the addition of protective agents to depress the melting point of the livers, which meant reducing the degree of supercooling. The standard clinical hypothermic preservation (HP) solution is University of Wisconsin (UW) solution, which we used as the base for our supercooling preservation solution. UW solution contains hydroxyethyl starch, raffinose and potassium lactobionate, which could modify ice nucleation and lower the melting point as compared with pure water (Supplementary Table 1). Potential toxicity of additional cryoprotective agents during prolonged high subzero preservation is an important consideration, which is why we had avoided them in our previous rat studies. Informed by our earlier work (see Methods) and literature, we chose two additives that are popular in cryopreservation but are not used in hypothermic organ preservation: (1) trehalose, for the protection of the extracellular compartment and to provide cell membrane stabilization at subzero temperatures[7], in addition to polyethylene glycol (PEG)[8] which was already present in our rat protocol; and (2) glycerol, which is freely permeable over plasma membranes[7] and therefore supplements 3-O-methyl-D-glucose (3-OMG), which accumulates intracellularly[4] and was a key additive for rat livers. Although glycerol is common in cryopreservation, the latest reports date back to the 70s and it has not been used for hypothermic or high subzero organ preservation in modern history[9].

Third was the loading scheme of the preservation cocktail. Although the melting point of the preservation solution was depressed by the addition of trehalose and to a greater extent by glycerol (Supplementary Table 1), the solution melting point does not fully reflect the melting point depression of the actual livers when loaded with that solution. The melting point of the preconditioned livers (Supplementary Fig. 2) was significantly ($P < 0.0001$, $t(13 \text{ degrees of freedom}) = 7.761$) higher (−2.1 °C) as compared with the preservation solution (−3.03 °C), which can potentially be explained by incomplete equilibration and a dilution effect of the preservation solution in the relatively large organ volume. While a 10 g rat liver can be simply flushed manually with a syringe, we experienced that the increased size of human grafts makes homogeneous loading of protective agents substantially harder, which initially resulted in freezing of the grafts. Uniform distribution of protective agents within the tissue is crucial in supercooled storage, since ice might initially nucleate at an insufficiently protected site and propagate through the entire organ. Also, the increased

[1]Center for Engineering in Medicine, Harvard Medical School & Massachusetts General Hospital, Boston, MA, USA. [2]Department of Surgery, University of Amsterdam, Amsterdam, the Netherlands. [3]Shriners Hospital for Children, Boston, MA, USA. [4]Department of Electron Microscopy Research, Theodor Bilharz Research Institute, Giza, Egypt. [5]Center for Transplant Sciences, Massachusetts General Hospital, Boston, MA, USA. *e-mail: kuygun@mgh.harvard.edu

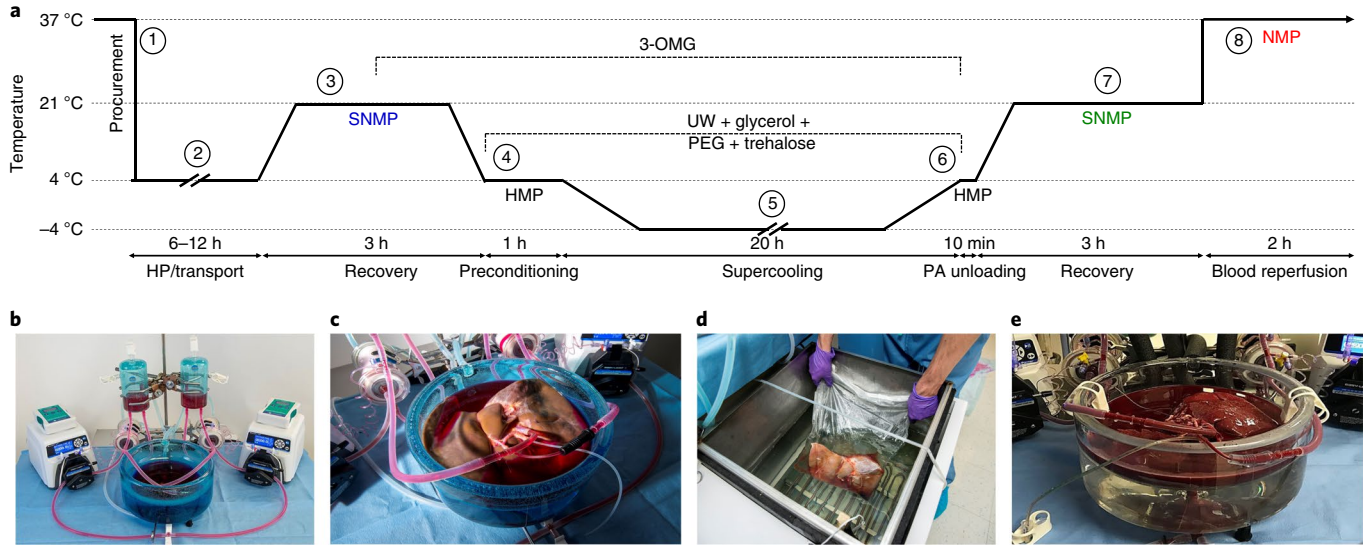

Fig. 1 | Outline of research design. a, Schematic temperature profile of the supercooling protocol: the overall research design comprises eight steps. (1) Five human livers, rejected for transplantation, were procured in standard fashion and (2) transported under HP conditions. (3) On arrival, we recovered the grafts from the incurred warm and cold ischemia and collected pre-supercooling viability parameters during 3 h of SNMP. We supplemented the perfusate with 19.42 g l^{-1} (200 mM) 3-OMG during the last hour of perfusion. (4) At the end of SNMP, we gradually lowered the perfusion temperature, which was followed by HMP with UW solution supplemented with 50 g l^{-1} (1.43 μM) 35 kDa PEG, 37.83 g l^{-1} (100 mM) trehalose dihydrate and 125.7 g l^{-1} (1.36 M) glycerol. (5) Following preconditioning with the protective agents, the livers were supercooled and stored free of ice at −4 °C for 20 h. (6) After supercooling, the protective agents were gradually washed out, and (7) the livers were recovered by SNMP, identical to pre-supercooling conditions except for addition of Trolox to the perfusate and absence of 3-OMG and cooling at the end of SNMP. Post-supercooling viability parameters were collected during SNMP and compared with their baseline values. (8) Three livers were additionally reperfused with non-leuko-reduced red blood cells and plasma at 37 °C as a model for transplantation. **b**, Machine perfusion system. **c**, Liver during SNMP recovery. **d**, Liver in supercooling basin of the chiller. **e**, Normothermic reperfusion with blood of the supercooled liver.

viscosity of the preservation solution due to the additional protective agents could potentially increase shear stress on the endothelium. The excessive shear stress can consequently cause substantial endothelial injury[10]. To address both concerns, we introduced an additional hypothermic machine perfusion (HMP) step to homogeneously precondition the organs and avert freezing during supercooling. Briefly, the liver was machine perfused at +4 °C, without recycling of the preservation medium. The preservative agent concentrations were increased gradually during HMP to avoid potential osmotic injury, and the perfusion flow rates and pressures were accurately compensated to account for the increase viscosity and avert endothelial injury.

Because subnormothermic machine perfusion (SNMP) after supercooling was critical for transplant survival in rats, we also chose this modality to recover the human livers after supercooling. Additional modifications related to engineering of the system to allow perfusion of human livers at multiple temperatures and in different configurations finally resulted in the human liver supercooling protocol that is outlined in Fig. 1 and described in detail in the Methods and Supplementary Fig. 3.

To assess whether supercooled human livers retained their viability, we took advantage of the fact that SNMP has been shown to allow detailed ex vivo assessment of liver viability[4,11–13]. To be able to control for donor-to-donor variability in the marginal human livers that were rejected for transplantation (Supplementary Table 2), we compared viability parameters during SNMP before and after supercooling (Fig. 2). Adenylate energy content, and, particularly, the organ's ability to recover it during (re)perfusion, is considered the most representative metric for liver viability[3,12,14–16]. The energy charge was low at the start of SNMP both before (that is, directly after HP) and after supercooling due to slowly ongoing vital cell processes during storage. In this regard, the glycerol in the supercooling preservation solution was potentially phosphorylated at the expense of ATP and ADP, contributing to the energy charge reduction during supercooling. Nonetheless, no statistical difference between pre- and post-supercooling energy charge was found (Fig. 2a and Supplementary Fig. 4a,b). Of note, the energy charge recovered significantly during SNMP ($P < 0.0001$, $F(1, 4$ degrees of freedom$) = 443.9$) both before and after supercooling ($P = 0.0209$, mean difference (95% confidence interval (95% CI)) = 0.190 (0.043 to 0.336), effect size of significant difference (η^2) = 0.75; and $P = 0.0185$, mean difference (95% CI) = 0.197 (0.050 to 0.343), $\eta^2 = 0.47$, respectively). The mean difference in end-SNMP energy charge was smaller than 20%. By comparison, >40% differences are observed in adenylate energy content between successful and unsuccessful transplanted livers in both large animal[15] and clinical[16–18] studies.

Additional important viability parameters during SNMP include bile production, vascular resistance and oxygen uptake, which were correlated to transplant survival after supercooling in rats[4]. Of these parameters, bile production has been clinically correlated to graft function after liver transplantation[18] and to human liver function during SNMP[12]. No statistically significant difference was found in bile production ($P = 0.433$, $F(1, 4) = 0.759$). Three livers produced the same amount of bile during SNMP before and after supercooling (Fig. 2b), indicating successful preservation. One liver (liver 2) did not produce bile either before or after supercooling and one liver (liver 1) stopped bile production after supercooling, while other viability parameters in both indicated preserved viability. Portal and arterial resistances (Fig. 2c) after supercooling were stable and no significant differences were found compared with pre-supercooling SNMP ($P = 0.649$, $F(1, 4) = 0.241$; and $P = 0.809$, $F(1, 4) = 0.067$, respectively). The maximal observed mean difference between portal vein resistance before and after supercooling was

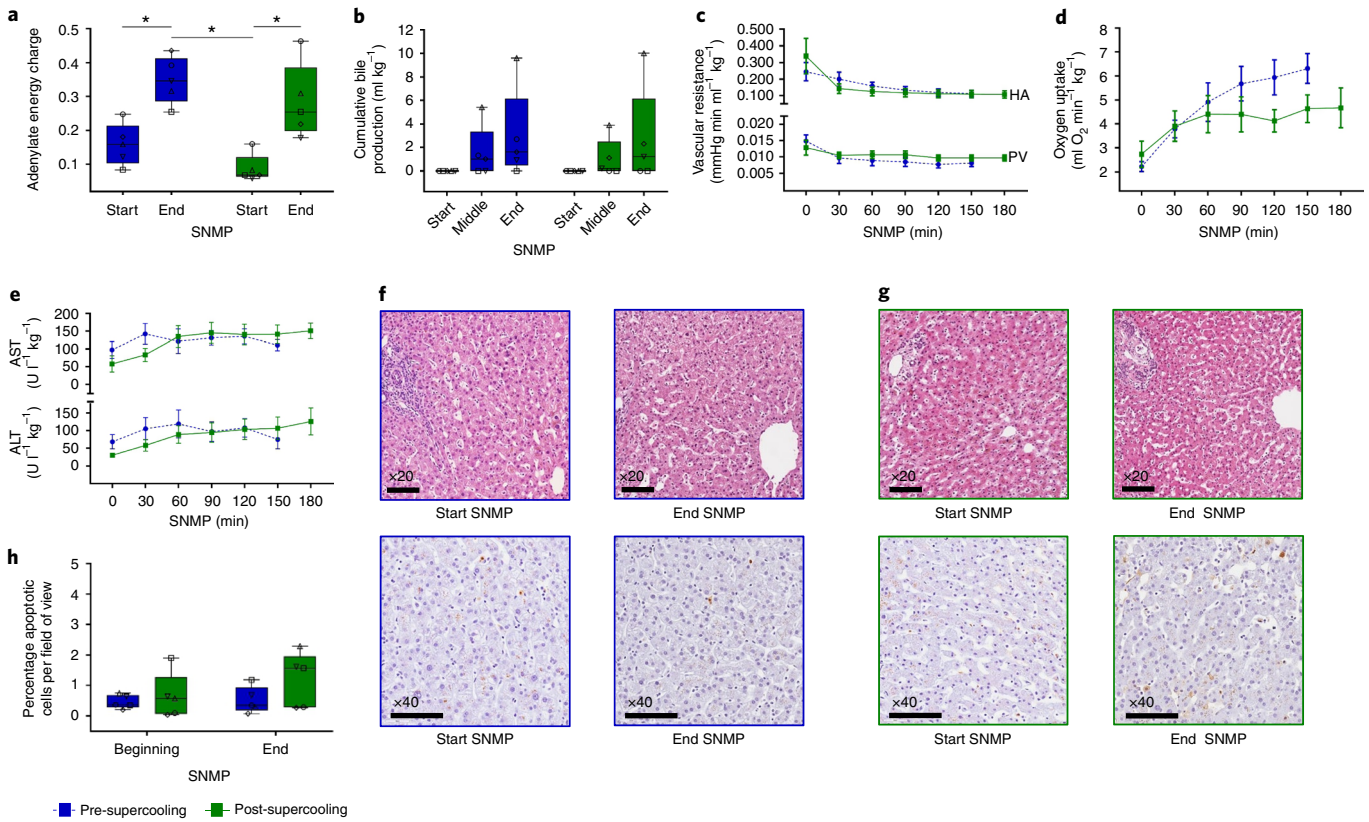

Fig. 2 | Key ex vivo viability parameters and histology during pre- and post-supercooling SNMP. a, Tissue adenylate energy charge showing recovery of energy charge after supercooling. Blue denotes pre-supercooling and green denotes post-supercooling throughout the figure. The symbols of the dot plot overlay correspond to the unique independent biological replicates ($n = 5$ throughout the figure) and match between Figs. 2 and 3; Supplementary Figs. 2, 4 and 5; and Supplementary Table 2. **b**, Cumulative bile production, also indicating full recovery and identical production after supercooling. **c**, Vascular resistance of the hepatic artery (HA) and the portal vein (PV), top and below, respectively, indicating no additional resistance in supercooled livers. **d**, Oxygen uptake rises and stabilizes similarly. **e**, AST and ALT concentrations in the perfusate, top and below, respectively, are effectively identical before and after supercooling, indicating no major cellular injury due to preservation. **f**, Light microscopy images of parenchymal liver biopsies during pre-supercooling SNMP. Top, hematoxylin and eosin staining. Bottom, staining for apoptotic DNA fragmentation by TUNEL. **g**, Light microscopy images of hematoxylin and eosin- (top) and TUNEL- (below) stained parenchymal liver biopsies during post-supercooling SNMP. **h**, Quantification of TUNEL-stained liver biopsies. Apoptotic cells were quantified per field of view of ~430 cells. There is a slight but not statistically significant increase in apoptotic cells during SNMP, which is similar before and after supercooled preservation. Asterisks denote statistical significance ($^*P < 0.05$, repeated measures two-way ANOVA followed by the Sidak multiple comparisons test). Boxes, median and interquartile range. Whiskers, minimum and maximum. Error bars of line graphs, mean ± s.e.m. Scale bars, 100 μm.

21% (at time (T) = 90 min), while much higher 100–150% increases are reported in the literature for nonviable livers[4,19]. The recovery in oxygen uptake rate at the start of SNMP was the same before and after supercooling. Although the oxygen uptake at the end of SNMP before supercooling was higher than the oxygen uptake at the end of SNMP after supercooling, the difference in oxygen uptake rate at individual time points did not reach statistical significance ($P = 0.272$, $F(1, 4) = 1.617$). To account for the initial recovery phase of oxygen uptake during the first 2 h of SNMP—which might attenuate a potential difference in the oxygen uptake at the end of perfusion—we also compared the oxygen uptake at the end of perfusion (area under the curve (AUC) at $T \geq 120$ min), which did not show a statistically significant difference ($P = 0.233$, $t(8) = 1.292$). The mean difference in total oxygen uptake (total AUC) before and after supercooling (Fig. 2d) was 17%, and three times lower than the reported 51% reduction in oxygen uptake (AUC) during SNMP of human livers with impaired viability[11].

Similar to bile production, lactate clearance is an important liver function that was observed both before and after supercooling (Supplementary Fig. 4c). Moreover, we found significantly higher lactate levels before supercooling ($P = 0.0105$, $F(5, 20) = 4.056$), which prevailed during the first hour of SNMP as compared with post-supercooling ($P = 0.0044$, mean difference (95% CI) = 2.714 (0.727 to 4.701), $\eta^2 = 0.42$ at $T = 30$ min; and $P = 0.0164$, mean difference (95% CI) = 2.326 (0.339 to 4.313), $\eta^2 = 0.17$ at $T = 60$ min, respectively) (Supplementary Fig. 4d). Since the livers were transported to our hospital under HP conditions, we hypothesize that the build-up of lactate during HP is higher, compared with supercooling, due to deeper metabolic stasis. As we observed this same pronounced trend in the liver donated after brain death (liver 4), this is unlikely to be solely due to warm ischemia during procurement of livers donated after circulatory death.

In addition to liver function and metabolism, we assessed liver injury before and after supercooling. Hepatocellular injury was the same and stable before and after supercooling as demonstrated by aspartate aminotransferase (AST), alanine aminotransferase (ALT) (Fig. 2e) and potassium (Supplementary Fig. 4e) concentrations in the perfusate. The transaminase levels we found are low compared with others[11,12,20–22], which could be explained by the 2 l perfusate that was nonrecirculated at the beginning of SNMP to wash out the protective agents. The stability of transaminase levels during perfusion is of particular importance since it confirms absence of

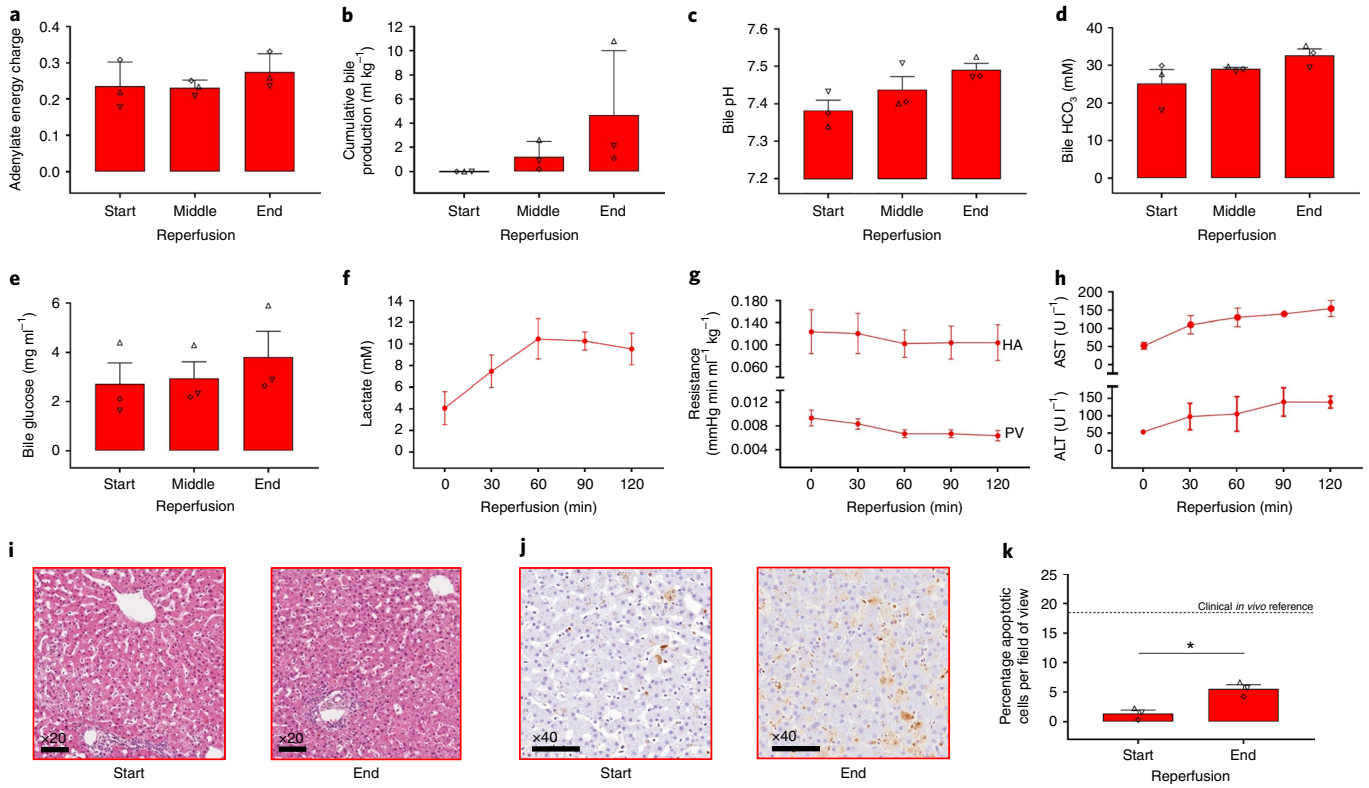

Fig. 3 | Key ex vivo viability parameters during simulated transplantation by normothermic blood reperfusion. a, Tissue adenylate energy charge at the start ($T = 0$ min), middle ($T = 60$ min) and end ($T = 120$ min) of reperfusion. The symbols of the dot plot overlay correspond to the unique independent biological replicates ($n = 3$ throughout the figure) and match between Figs. 2 and 3; Supplementary Figs. 2, 4 and 5; and Supplementary Table 2. **b**, Cumulative bile production. **c**, Bile pH. **d**, Bile HCO_3^- concentration. **e**, Bile glucose concentration. **f**, Lactate concentrations of the arterial inflow. **g**, Vascular resistance of the HA and the PV, top and below, respectively. **h**, AST and ALT concentrations in the plasma, top and below, respectively. **i**, Light microscopy images of parenchymal liver biopsies during reperfusion stained with hematoxylin and eosin. **j**, Light microscopy images of parenchymal liver biopsies during reperfusion stained for apoptotic DNA fragmentation by TUNEL. **k**, Quantification of TUNEL-stained liver biopsies. Apoptotic cells were quantified per field of view of ~430 cells. The horizontal dashed line represents the reported range of TUNEL-positive cells in biopsies taken directly after full reperfusion in vivo during liver transplantation[29]. Asterisk denotes statistical significance (*$P = 0.009$, paired two-tailed Student's *t*-test). Error bars, mean ± s.e.m. Scale bars, 100 μm.

potential toxicity of the protective agents. This is confirmed by histology (Fig. 2f,g), which shows preserved lobular architecture with viable hepatocytes and intact sinusoidal endothelial cells. No necrosis or substantial increase in apoptotic cells was observed (Fig. 2h), and pre-existing focal signs of hepatocellular and endothelial injury were marginally aggravated during preservation. In summary, we find that the human livers tested displayed no substantial difference in viability before and after extended subzero supercooling preservation. Although the differences in energy charge, oxygen uptake and apoptosis were not significant and small compared with referenced literature, they should be further investigated, aiming to improve supercooling preservation.

With initial success of our supercooling protocol, we then subjected three livers to additional ex vivo normothermic reperfusion with blood as a model for transplantation[16,23] (Figs. 1e and 3). Unlike normothermic machine perfusion (NMP), which is intended to assess and improve liver viability, the blood used in reperfusion studies contains white blood cells, platelets and complement, which are key components of ischemia reperfusion injury. This fundamental difference should be taken into account when we compare the viability parameters during reperfusion after supercooling with NMP data in the literature after HP, which does not include the immunologic components. Accessibility of whole blood in sufficient quantities for human liver reperfusion studies is severely limited. Therefore, we recombined red blood cells and fresh frozen plasma instead. Although this is suboptimal to the use of fresh whole blood, we specifically used non-leuko-reduced blood products and confirmed the presence of white blood cells and platelets (Supplementary Table 3).

During blood reperfusion, the livers had a stable energy charge (Fig. 3a and Supplementary Fig. 5a,b). Moreover, the mean energy charge was higher after just 7 h of HP than we previously found in both ex vivo studies and directly after reperfusion in transplanted human livers[16]. The stability of energy charge during reperfusion is of additional importance, since a drop after initial restoration of energy charge during clinical reperfusion was significantly correlated with early allograft dysfunction[16]. This could potentially be explained by mitochondrial function that cannot keep up with the increased energy demand after the transition from a reduced to a full metabolic rate during normothermic reperfusion. Together with the increased oxygen consumption (Supplementary Fig. 5c), the stable energy charge indicates preserved mitochondrial function after supercooling preservation.

The higher metabolic rate during normothermic reperfusion resulted in increased liver function, reflected by bile and urea production and lactate metabolism. Bile (Fig. 3b) production increased as compared with SNMP and the resulting cumulative bile production volumes (per liver weight) correspond to the range of values reported in the literature during NMP of transplanted[22,24,25] and non-transplanted[20–22] livers. Bile pH, HCO_3^- and glucose are increasingly

acknowledged as important parameters of biliary function during NMP. The mean bile pH (Fig. 3c) and the bile HCO_3^- (Fig. 3d) at the end of reperfusion respectively reached and surpassed the suggested criteria for transplantable liver viability[22,26]. Although the bile glucose concentrations during reperfusion (Fig. 3e) were higher than proposed clinical transplantable criteria, they were the same as reported for research-quality livers by others[22]. Notably, these livers were perfused after much shorter clinically used durations of HP. Urea production (Supplementary Fig. 5d) also increased as a result of the increased metabolic rate and was higher than reported by others during NMP in both ex vivo[20] and clinical studies[27], indicating preserved liver function. Similar to others during NMP[16,20,22,24,25], we observed a rise in lactate during the first hour of reperfusion and subsequent clearance (Fig. 3f and Supplementary Fig. 5e). It should be considered that the livers in this study were initially rejected for transplantation, and the confidence intervals of the lactate concentration at the end of reperfusion largely overlap with time-matched values reported by others during NMP of rejected human livers[20,28].

In addition to liver function and metabolism, we assessed liver injury during simulated transplantation. Absolute values of vascular resistance are dependent on machine perfusion modality and values that correspond to viability remain to be sustained. However, stable resistance profiles as we found during reperfusion (Fig. 3g) are favorable, since increasing resistance may reflect endothelial injury and hepatocellular edema as a measure of decreasing viability. The early increase in AST and ALT (Fig. 3h) during the first half-hour of reperfusion is less than we expected based on reported AST and ALT levels during NMP in literature[20–22,24,27]. Histology after reperfusion (Fig. 3i,j) shows preserved lobular architecture with patches of reversible hepatocellular injury in the form of hepatocellular edema and hydropic changes. Focal spots of hepatocyte dropout with loss of sinusoidal endothelial cells were observed in the pericentral zone and were markedly correlated to the initial histology of the liver graft, suggesting that the pre-existing injury of the marginal grafts was aggravated during reperfusion. We found a significant ($P=0.009$, $t(2)=32.89$) increase in apoptotic cells to a percentage of 5.5% (Fig. 3k), while over 15% is normally the case directly after full reperfusion in vivo during transplantation[29]. It should be noted that apoptosis can continue to develop beyond the 2-h time course that is covered by both our ex vivo reperfusion model and the peroperative reference during clinical liver transplantation. Limited (hepato) cellular injury is furthermore confirmed by decreasing potassium after the first half our of reperfusion (Supplementary Fig. 5f).

In this study, we showed the feasibility of subzero human organ preservation using discarded human livers. To achieve this, we developed a multi-temperature perfusion protocol, featuring practical steps to minimize air–liquid interfaces, and repurposed protective agents to stabilize the supercooled state of a large aqueous volume, which was crucial to prevent human livers from freezing during supercooling. We validated our approach with viability assessment of the grafts during SNMP before and after supercooling and by normothermic reperfusion with blood as a model for transplantation. Formally, this model can only suggest the adequacy of supercooling preservation. However, in the case of preclinical human tissue studies, ex vivo viability assessment during machine perfusion has a strong theoretical background and is supported by experimental and clinical transplantation studies: these all indicate that supercooled human grafts retained their viability despite substantially extended preservation as compared with the clinical standard. Moreover, we observed parameters indicating viability during simulated transplantation of marginal livers up to 44 h after procurement.

While we limited this feasibility study to −4 °C, further optimization of the supercooling protocol could potentially reduce the ice-free storage temperature. Also, reduction or substitution of the glycerol in the supercooling preservation solution might be beneficial to avert potential glycerol phosphorylation during supercooling. Both might lower the rate of ATP depletion during supercooling and consequently increase the preservation duration. Rewarming perfusion is a key step in reducing reperfusion injury after supercooling, and may benefit further from either new machine perfusion modalities used in clinical trials or emerging approaches in ensuring optimum rewarming temperatures[30]. The use of human livers makes this study clinically relevant and promotes the translation of subzero organ preservation to the clinic. However, long-term survival experiments of transplanted supercooled livers in swine or an alternative large animal model will be needed before clinical translation.

Online content

Any methods, additional references, Nature Research reporting summaries, source data, statements of code and data availability and associated accession codes are available at https://doi.org/10.1038/s41587-019-0223-y.

Received: 26 October 2018; Accepted: 12 July 2019;
Published online: 09 September 2019

References

1. Giwa, S. et al. The promise of organ and tissue preservation to transform medicine. *Nat. Biotechnol.* **35**, 530–542 (2017).
2. Buying time for transplants. *Nat. Biotechnol.* **35**, 801 (2017).
3. Bruinsma, B. G. & Uygun, K. Subzero organ preservation: the dawn of a new ice age? *Curr. Opin. Organ Transplant.* **22**, 281–286 (2017).
4. Berendsen, T. A. et al. Supercooling enables long-term transplantation survival following 4 days of liver preservation. *Nat. Med.* **20**, 790–793 (2014).
5. Bruinsma, B. G. et al. Supercooling preservation and transplantation of the rat liver. *Nat. Protoc.* **10**, 484–494 (2015).
6. Huang, H., Yarmush, M. L. & Usta, O. B. Long-term deep-supercooling of large-volume water and red cell suspensions via surface sealing with immiscible liquids. *Nat. Commun.* **9**, 3201 (2018).
7. Storey, K. B. & Storey, J. M. Molecular biology of freezing tolerance. *Compr. Physiol.* **3**, 1283–1308.
8. Dutheil, D., Underhaug Gjerde, A., Petit-Paris, I., Mauco, G. & Holmsen, H. Polyethylene glycols interact with membrane glycerophospholipids: is this part of their mechanism for hypothermic graft protection? *J. Chem. Biol.* **2**, 39–49 (2009).
9. Jacobsen, I. A., Pegg, D. E., Wusteman, M. C. & Robinson, S. M. Transplantation of rabbit kidneys perfused with glycerol solutions at 10 degrees C. *Cryobiology* **15**, 18–26 (1978).
10. 't Hart, N. A. et al. Determination of an adequate perfusion pressure for continuous dual vessel hypothermic machine perfusion of the rat liver. *Transpl. Int.* **20**, 343–352 (2007).
11. Bruinsma, B. G. et al. Subnormothermic machine perfusion for ex vivo preservation and recovery of the human liver for transplantation: subnormothermic machine perfusion of human livers. *Am. J. Transplant.* **14**, 1400–1409 (2014).
12. Bruinsma, B. G. et al. Metabolic profiling during ex vivo machine perfusion of the human liver. *Sci. Rep.* **6**, 22415 (2016).
13. Sridharan, G. V. et al. Metabolomic modularity analysis (MMA) to quantify human liver perfusion dynamics. *Metabolites* **7**, 58 (2017).
14. Vajdová, K., Graf, R. & Clavien, P.-A. ATP-supplies in the cold-preserved liver: a long-neglected factor of organ viability. *Hepatology* **36**, 1543–1552 (2002).
15. Higashi, H., Takenaka, K., Fukuzawa, K., Yoshida, Y. & Sugimachi, K. Restoration of ATP contents in the transplanted liver closely relates to graft viability in dogs. *Eur. Surg. Res.* **21**, 76–82 (1989).
16. Bruinsma, B. G. et al. Peritransplant energy changes and their correlation to outcome after human liver transplantation. *Transplantation* **101**, 1637–1644 (2017).
17. Lanir, A. et al. Hepatic transplantation survival: correlation with adenine nucleotide level in donor liver. *Hepatology* **8**, 471–475 (1988).
18. Kamiike, W. et al. Adenine nucleotide metabolism and its relation to organ viability in human liver transplantation. *Transplantation* **45**, 138–143 (1988).
19. Bruinsma, B. G., Berendsen, T. A., Izamis, M.-L., Yarmush, M. L. & Uygun, K. Determination and extension of the limits to static cold storage using subnormothermic machine perfusion. *Int. J. Artif. Organs* **36**, 775–780 (2013).
20. op den Dries, S. et al. Ex vivo normothermic machine perfusion and viability testing of discarded human donor livers: normothermic perfusion of human livers. *Am. J. Transplant.* **13**, 1327–1335 (2013).

21. Sutton, M. E. et al. Criteria for viability assessment of discarded human donor livers during ex vivo normothermic machine perfusion. *PloS ONE* **9**, e110642 (2014).
22. Watson, C. J. E. et al. Observations on the ex situ perfusion of livers for transplantation. *Am. J. Transplant.* https://doi.org/10.1111/ajt.14687 (2018).
23. Avruch, J. H. et al. A novel model for ex situ reperfusion of the human liver following subnormothermic machine perfusion. *Technology* **05**, 196–200 (2017).
24. Bral, M. et al. Preliminary single-center Canadian experience of human normothermic ex vivo liver perfusion: results of a clinical trial. *Am. J. Transplant.* **17**, 1071–1080 (2017).
25. Mergental, H. et al. Transplantation of declined liver allografts following normothermic ex-situ evaluation. *Am. J. Transplant.* **16**, 3235–3245 (2016).
26. Matton, A. P. M. et al. Biliary bicarbonate, pH and glucose are suitable biomarkers of biliary viability during ex situ normothermic machine perfusion of human donor livers. *Transplantation* https://journals.lww.com/transplantjournal/fulltext/2019/07000/Biliary_Bicarbonate,_pH,_and_Glucose_Are_Suitable.21.aspx (2018).
27. Reiling, J. et al. Urea production during normothermic machine perfusion: price of success? *Liver Transpl.* **21**, 700–703 (2015).
28. Westerkamp, A. C. et al. Oxygenated hypothermic machine perfusion after static cold storage improves hepatobiliary function of extended criteria donor livers. *Transplantation* **100**, 825–835 (2016).
29. Borghi-Scoazec, G. et al. Apoptosis after ischemia-reperfusion in human liver allografts. *Liver Transpl. Surg.* **3**, 407–415 (1997).
30. Manuchehrabadi, N. et al. Improved tissue cryopreservation using inductive heating of magnetic nanoparticles. *Sci. Transl. Med.* **9**, eaah4586 (2017).

Acknowledgements

Funding from the US National Institutes of Health (NIH) (grant nos. R01DK096075, R01DK107875 and R01DK114506) and the Department of Defense (contract no. RTRP W81XWH-17-1-0680) are gratefully acknowledged. We thank Sylvatica Biotech, Inc. and are grateful for support through the NIH (grant no. R21EB023031) and the US Army MRDC (contract no. W81XWH-16-C-0067). R.J.V. acknowledges a stipend from the Michael van Vloten Fund for Surgical Research. S.N.T. acknowledges support from NIH grant no. K99 HL143149. We thank M. Karabacak, Y.M. Yu and F. Lin at the Mass Spectrometry Core Facility (Shriners Hospital for Children, Boston, MA) for assistance with adenylate quantification. We thank L. Burlage, A. Matton, B. Bruinsma and C. Pendexter for experimental assistance. Finally, appreciation is extended to LiveOnNY, and we are especially grateful for our collaboration with New England Donor Services and their generous support that enables research with human donor organs. The views, opinions and/or findings contained in this manuscript are those of the authors and should not be construed as an official position, policy or decision of any of the institutions that supported the research, unless so designated by other documentation.

Author contributions

R.J.V., S.N.T. and K.U. conceived and designed the study. R.J.V., P.D.B., S.N., S.E.J.C. and S.O. performed data acquisition. R.J.V., S.N.T., E.O.A.H., H.Y., M.L.Y., J.F.M., M.T. and K.U. analyzed and interpreted data. R.J.V., S.N.T. and S.O. designed and constructed the perfusion and supercooling system. R.J.V., S.N.T. and K.U. wrote the manuscript. R.J.V., S.N.T., E.O.A.H., T.M.G., M.L.Y., J.F.M., M.T., H.Y. and K.U. participated in critical revision of the manuscript for intellectual content. R.J.V., S.N.T. and K.U. performed statistical analysis. All authors contributed to the preparation of the manuscript.

Competing interests

The authors declare competing financial interests. M.T., M.L.Y., R.J.V., K.U. and S.N.T. have provisional patent applications relevant to this study. K.U. has a financial interest in Organ Solutions, a company focused on developing organ preservation technology. Authors' interests are managed by MGH and Partners HealthCare in accordance with their conflict of interest policies.

Additional information

Supplementary information is available for this paper at https://doi.org/10.1038/s41587-019-0223-y.

Correspondence and requests for materials should be addressed to K.U.

Methods

Organ acquisition. Approval from the institutional review board was obtained before any experiments involving the human organs were performed. Human livers were procured in standard fashion[11] by the organ procurement organizations New England Donor Services Bank and LiveOnNY. Informed consent was obtained from the donors by the organ procurement organization. After the livers were rejected for transplantation, they were transported to our laboratory under conventional HP conditions in UW solution. We excluded livers based on the following criteria: warm ischemic time > 60 min, cold ischemic time > 18 h, >20% macro steatosis, donor history of liver fibrosis and any grade of liver laceration.

Additives for supercooling. Selection of additivities to enable supercooled preservation of human livers was informed by our earlier studies and literature. We found 35 kDa PEG and 3-OMG to be essential ingredients in our previous rat protocol[5]. As they proved insufficient in scaling up to human livers, we relied on our experience with additives in other biopreservation studies (please note that these earlier studies were not supercooling experiments, and instead focused on traditional cryopreservation, and other high-subzero approaches that do involve freezing, in various formats). We considered additives including dextrose, glucose, sucrose, dimethylsulfoxide, PEG at 8 kDa and 35 kDa, glutathione and vitamin E, as well as glycerol and trehalose, based on their hepatoxicity and post-preservation viability profiles (typically live/dead assay and occasionally ALT release). Based on these insights we proceeded with glycerol and trehalose for testing in human livers, as detailed in the text.

Reagents. Exact compositions of the perfusates and storage solution can be found in Supplementary Table 4. In short, two recovery perfusates (pre-supercooling recovery solution and post-supercooling recovery solution) were made for SNMP recovery after HP and supercooling. Both were composed of 4 l modified Williams' medium E (Sigma Aldrich) and were exactly the same, except for the addition of Trolox (Cayman Chemical Company) to the post-supercooling recovery solution. For stepwise protective agent loading, two loading solutions (loading solution 1 and loading solution 2) were made, which respectively were composed of 1 l and 3 l UW solution (Bridge to Life) supplemented with 35 kDa PEG (Sigma Aldrich), D-(+)-trehalose dihydrate (Sigma Aldrich) and glycerol (ThermoFisher Scientific). For the stepwise protective agent unloading, 1 l modified Williams' medium E was supplemented with PEG, trehalose and glycerol. For blood reperfusion, 3 units of non-leuko-reduced type O Rh^+ packed red blood cells (Research Blood Components) were combined with 3 units of non-leuko-reduced type O Rh^+ fresh frozen plasma (Research Blood Components) and supplemented with modified Williams' medium E to a total volume of 4 l. The perfusates were refrigerated at 4 °C and the blood was warmed to 37 °C before use. The pH of all solutions was corrected to a pH between 7.3 and 7.4, by addition of $NaHCO_3$, before priming the perfusion system.

Machine perfusion and supercooling system. The machine perfusion system consists of a duplex nonpulsatile circulation, providing portal and arterial perfusion (see Fig. 1b). The liver drains freely in a jacketed organ chamber that also serves as perfusate reservoir (Radnoti). For both portal and arterial circulation, the perfusate is pumped by a flow rate-controlled roller pump (Cole Palmer) through a heat exchanger combined with a hollow fiber oxygenator (LivaNova), a jacketed bubble trap (Radnoti), a pressure sensor (Living Systems Instrumentation) and a sampling port (Cole Palmer), which are connected in series with size 24 silicone tubing (Cole Palmer). The two membrane oxygenators are oxygenated by a combined flow of 2 l min^{-1} with a mixture of 95% O_2 and 5% CO_2. Both bubble traps are filled to 25% and therefore also serve as compliance chambers to minimize pressure pulses created by the roller pumps. The system contains perfusate in- and outflows, which can be configured to either recirculation perfusion or single-pass perfusion. The liver and perfusate temperatures are controlled by a separate warming/cooling circuit. Water or refrigerant is either warmed by a warm water bath (ThermoFisher Scientific) or cooled by a chiller (Optitemp), respectively, and pumped through the heat exchangers and the jackets of the bubble traps and the organ chamber. The chiller contains a 75 l refrigerant basin that also holds the liver during supercooling.

Protocol. While the graft was submerged in ice-cold UW, the common bile duct, hepatic artery and portal vein were dissected. Side branches were identified and tied using 2.0 silk sutures. Subsequently, the cystic duct and artery were dissected, tied and cut distally from the suture. Next, the gallbladder and diaphragm were removed. Cannulas were inserted in the common bile duct, hepatic artery and portal vein (Organ Assist) and secured in place by 1.0 silk sutures. Lastly, the liver was flushed with 1.5 l and 0.5 l ice-cold Ringer's lactate through the portal vein and hepatic artery, respectively, to remove the UW solution. The vasculature was checked for leaks during the flush, which were tied or repaired with 2.0 silk or 5.0 prolene sutures accordingly.

The machine perfusion system was primed with the pre-supercooling recovery solution and the machine perfusion system in- and outflow were configured in single-pass perfusion. The warm water bath was set at 21 °C and connected to the cooling/rewarming circuit. The prepared liver was placed in the organ chamber and the cannulas were de-aired and connected to the perfusion system. Perfusion was initiated by starting the pumps at 50 ml min^{-1}. The flow rates were manually adjusted to obtain perfusion pressures of 5 mmHg and 60 mmHg for the portal vein and hepatic artery, respectively. The bile duct cannula was connected to a collection reservoir and a needle thermocouple (Omega) was inserted in the right lobe. After 2 l perfusate was passed through the liver, the machine perfusion system was configured from the single-pass to recirculation perfusion and the remaining 2 l recovery solution was recirculated throughout the perfusion. The liver was gradually rewarmed during the first 30 min of perfusion. After 90 min of perfusion, regular insulin (Massachusetts General Hospital Pharmacy) and 3-OMG (Sigma Aldrich) were added to the perfusate. After 150 min, the perfusate and liver were gradually cooled to 4 °C in 30 min, by connecting the cooling/rewarming circuit to the chiller. Perfusion pressures were lowered to 3 mmHg and 30 mmHg during HMP. After gradual cooling, the machine perfusion system was configured into single-pass perfusion and the livers were perfused with 1 l loading solution 1, followed by 3 l loading solution 2.

Following preconditioning during HMP, the liver was disconnected from the machine perfusion system and bagged in a Steri-Drape Isolation Bag (3M Healthcare). Before the bag was closed, all air and residual loading solution were removed. The bagged liver was suspended and fully submerged in the chiller basin and supercooling was initiated by setting the chiller temperature to −4 °C. The chiller temperature was regularly checked during supercooling. After 20 h of supercooling, the liver was removed from the chiller basin. To confirm that none of the livers froze during supercooling, the livers were visually inspected, and the soft liver tissue manually palpated when they were removed from the bag.

After the liver was removed from the bag it was connected to the machine perfusion system. Post-supercooling SNMP was identical to pre-supercooling machine perfusion except for the following points: (1) Hypothermic single-pass perfusion of 1 l unloading solution preceded the single-pass perfusion of 2 l recovery solution. Similar to pre-supercooling SNMP, the start of perfusion with recovery solution was defined as start of perfusion. (2) Perfusion was continued for 180 min at 21 °C instead of cooling, before supercooling after 150 min perfusion. (3) The antioxidant Trolox was added to the perfusate. (4) No 3-OMG or insulin was added to the perfusate.

The temperature of the warm water bath was set from 21 °C to 38 °C to warm the liver core temperature to 37 °C within 15 min. Meanwhile, the single-pass perfusion configuration of the perfusion system was used to replace the 2 l recovery solution with 2 l warm blood, which was recirculated during 2 h reperfusion. Target pressures of 5 mmHg and 60 mmHg were used for the portal vein and hepatic artery, respectively.

Viability analysis. The livers were weighed before pre-supercooling SNMP and after either post-supercooling SNMP or blood reperfusion. One liver was weighed after both pre-supercooling SNMP and reperfusion (liver 3). Hepatic artery and portal vein flow rates and pressures were registered every 30 min during perfusions and reperfusion.

Real-time perfusate and blood measurements were performed every 30 min; pH, pO_2, HCO_3^- and lactate were measured in the portal vein, hepatic artery and vena cava, and Na, K, Ca, Cl, glucose and Hb were measured in the perfusate reservoir, using an Istat blood analyzer (Abbot Laboratories). Whole blood counts were performed during reperfusion of one liver (liver 5) using a Cell Dyn Emerald Hematology Analyzer (Abbot Laboratories). Every 30 min, additional 5 ml perfusate samples or plasma samples were collected, immediately frozen on dry ice and stored at −80 °C for post hoc analysis of AST, ALT and urea, using colorimetric kits (ThermoFisher Scientific) according to the manufacturer's instructions.

Bile volume in the bile reservoir was measured and collected at the start, middle and end of SNMP and blood reperfusion.

Bilateral wedge biopsies were taken right before and at the end of SNMP, and halfway through and at the end of blood reperfusion. Biopsies were fixed in buffered 5% formaldehyde for 24 h and stored in 70% ethanol until outsourced processing and staining for hematoxylin and eosin and terminal deoxynucleotidyl transferase dUTP nick end labeling (TUNEL) staining (Massachusetts General Hospital Histology Molecular Pathology Core). Hematoxylin and eosin-stained slides were blindly assessed by an experienced liver pathologist (E.O.A.H). Processed TUNEL slides were scanned under ×40 magnification using an Aperio ImageScope (Leica Biosystems). For quantification of TUNEL histology, positive cells were counted in three sections of 450 μm^2 per slide at standardized locations (at 50% on the radius from the center to the edge of the slide at 0°, 60° and 120°) by two independent and blinded measurers. Sections of the wedge biopsies (~1 g) were flash frozen in liquid nitrogen and stored at −80 °C. Adenosine triphosphate (ATP), adenosine diphosphate (ADP), adenosine monophosphate (AMP) and nicotinamide adenine dinucleotide (NAD^+ and NADH) were determined as described elsewhere[12]. In short, the tissue was homogenized in liquid nitrogen and analyzed with targeted multiple reaction monitoring on a 3200 triple quadrupole liquid chromatography-mass spectrometry system (AB Sciex).

To measure the solution melting point, a thin (0.2 mm wire diameter) K-type thermocouple wire (Omega) was inserted together with the sample in a glass capillary (2.0 mm diameter). The sample was flash frozen and thawed at constant ambient temperature (4 °C) while the temperature was logged at 100 ms intervals

using a USB Thermocouple Data Acquisition Module (Omega) and Picolog 6 (Picotech) software. The melting point was derived from the horizontal asymptote of the melting temperature profile.

To measure the melting point of the livers, flash-frozen tissue biopsies taken before pre- and post-supercooling SNMP were used. The tissue was crushed in liquid nitrogen and loaded in the glass capillary. The melting point was measured following the same procedure as described for the solutions.

Data processing. To calculate vascular resistance, the perfusion pressure was divided by the corresponding flow rate and initial liver weight.

Energy charge was calculated with the following formula: ATP + 0.5ADP/(ATP + ADP + AMP).

Oxygen consumption was calculated with the following formula: (aO2*(art_pO2*art_flow + Port_pO2*port_flow − ven_pO2*(art_flow + port_flow)) + Hb*cHb* (art_sO2/100*art_flow + port_sO2/100*port_flow − ven_sO2/100*(art_flow + port_flow)))/liver_weight. Where aO2 is oxygen solubility coefficient (3.14×10^{-5} ml O_2 per mmHgO_2 per ml); art_pO2 is arterial partial oxygen pressure (mmHg); port_pO2 is portal partial oxygen pressure (mmHg); ven_pO2 is venous partial oxygen pressure (mmHg); art_flow is arterial flow rate (ml min^{-1}); port_flow is portal flow rate (ml min^{-1}); art_sO2 is arterial hemoglobin saturation (%); port_sO2 is portal hemoglobin saturation (%); ven_sO2 is venous hemoglobin saturation (%); cHb is hemoglobin oxygen-binding capacity (1.34 ml O_2 g^{-1}); Hb is hemoglobin (g ml^{-1}); and liver_weight is liver weight (kg).

Lactate clearance was calculated with the following formula: art_lactate*art_flow + port_lactate*port_flow-ven_lactate*(art_flow + port_flow). Where art_lactate is arterial lactate concentration (mM); port_lactate is portal lactate concentration (mM); and ven_lactate is vebous lactate concentration (mM).

In one case (liver 1), missing portal blood gas values were replaced by the arterial values to calculate oxygen uptake and lactate clearance.

Statistical analyses. Statistical analysis was performed in Prism 7.03 (GraphPad Software). Pre- and post-supercooling SNMP data ($n = 5$) and reperfusion data ($n = 3$) were obtained during independent supercooling experiments using five unique human livers (Supplementary Table 2). Data were analyzed for normal distribution by visual inspection and the Shapiro–Wilk normality test. Repeated measures two-way analysis of variance (ANOVA), with the Sidak multiple comparisons test, was used for comparison of the time-course perfusion data. The percentages of TUNEL-positive cells at the start and end of reperfusion were compared with paired two-tailed Student's *t*-tests. Total oxygen consumption was calculated by AUC analysis and compared with two-tailed Student's *t*-tests. The melting points of liver tissues (obtained during the $n = 5$ independent supercooling experiments) and solutions were compared using paired and nonpaired two-tailed Student's *t*-tests, respectively. The η^2 values were calculated in Office Excel (Microsoft) using the statistical output from Prism. *P* values smaller than 0.05 were considered statistically significant. The summary statistics (*F* and *t* values) are provided in the text, accompanied by the corresponding degrees of freedom in parentheses. Further information on research design is available in the Nature Research Reporting Summary linked to this article.

Reporting Summary. Further information on research design is available in the Nature Research Reporting Summary linked to this article.

Data availability

The authors declare that the data supporting the findings of this study are available within the paper and its supplementary information files. Any additional data if needed will be provided upon reasonable request.

nature research

Corresponding author(s): Korkut Uygun

Last updated by author(s): 06-21-2019

Reporting Summary

Nature Research wishes to improve the reproducibility of the work that we publish. This form provides structure for consistency and transparency in reporting. For further information on Nature Research policies, see Authors & Referees and the Editorial Policy Checklist.

Statistics

For all statistical analyses, confirm that the following items are present in the figure legend, table legend, main text, or Methods section.

n/a	Confirmed	
☐	☒	The exact sample size (*n*) for each experimental group/condition, given as a discrete number and unit of measurement
☐	☒	A statement on whether measurements were taken from distinct samples or whether the same sample was measured repeatedly
☐	☒	The statistical test(s) used AND whether they are one- or two-sided *Only common tests should be described solely by name; describe more complex techniques in the Methods section.*
☒	☐	A description of all covariates tested
☐	☒	A description of any assumptions or corrections, such as tests of normality and adjustment for multiple comparisons
☐	☒	A full description of the statistical parameters including central tendency (e.g. means) or other basic estimates (e.g. regression coefficient) AND variation (e.g. standard deviation) or associated estimates of uncertainty (e.g. confidence intervals)
☐	☒	For null hypothesis testing, the test statistic (e.g. *F*, *t*, *r*) with confidence intervals, effect sizes, degrees of freedom and *P* value noted *Give P values as exact values whenever suitable.*
☒	☐	For Bayesian analysis, information on the choice of priors and Markov chain Monte Carlo settings
☒	☐	For hierarchical and complex designs, identification of the appropriate level for tests and full reporting of outcomes
☐	☒	Estimates of effect sizes (e.g. Cohen's *d*, Pearson's *r*), indicating how they were calculated

Our web collection on statistics for biologists contains articles on many of the points above.

Software and code

Policy information about availability of computer code

Data collection	Data was collected in Microsoft Excel 365
Data analysis	Data was analysis was performed in GraphPad Prism 7

For manuscripts utilizing custom algorithms or software that are central to the research but not yet described in published literature, software must be made available to editors/reviewers. We strongly encourage code deposition in a community repository (e.g. GitHub). See the Nature Research guidelines for submitting code & software for further information.

Data

Policy information about availability of data

All manuscripts must include a data availability statement. This statement should provide the following information, where applicable:

- Accession codes, unique identifiers, or web links for publicly available datasets
- A list of figures that have associated raw data
- A description of any restrictions on data availability

The data supporting the findings of this study are available within the paper and its supplementary information files. Any additional data if needed will be provided upon request.

Field-specific reporting

Please select the one below that is the best fit for your research. If you are not sure, read the appropriate sections before making your selection.

☒ Life sciences ☐ Behavioural & social sciences ☐ Ecological, evolutionary & environmental sciences

Life sciences study design

All studies must disclose on these points even when the disclosure is negative.

Sample size	The goal of this proof of concept study was to demonstrate that subzero organ preservation by supercooling of human livers is possible. Therefore, no sample size calculations were performed. Given the limited availability of discarded human donor livers, we used 5 consecutively offered livers that matched the inclusion criteria to demonstrate feasibility and repeatability of supercooling preservation.
Data exclusions	No data were excluded.
Replication	Reproducibility of supercooling preservation is ensured by 5 consecutive experiments using human livers that were rejected for transplantation and met the inclusion criteria of this study. All attempts at replication were succesfull and the data of all 5 repetitions are included in the manuscript.
Randomization	Randomization of group allocation was not relevant for this study since the research design consists of one experimental group that contains a pre- and post-preservation viability measurement.
Blinding	Blinding to group allocation was not relevant for this study since the research design consists of one experimental group that contains a pre and post-preservation viability measurement. Data analysis was blinded where appropriate; i.e. histology assessment and quantification.

Reporting for specific materials, systems and methods

We require information from authors about some types of materials, experimental systems and methods used in many studies. Here, indicate whether each material, system or method listed is relevant to your study. If you are not sure if a list item applies to your research, read the appropriate section before selecting a response.

Materials & experimental systems

n/a	Involved in the study
☒	☐ Antibodies
☒	☐ Eukaryotic cell lines
☒	☐ Palaeontology
☒	☐ Animals and other organisms
☐	☒ Human research participants
☒	☐ Clinical data

Methods

n/a	Involved in the study
☒	☐ ChIP-seq
☒	☐ Flow cytometry
☒	☐ MRI-based neuroimaging

Human research participants

Policy information about studies involving human research participants

Population characteristics	The mean donor age was 52 years, ranging from 32 to 60. 20% of the donors were male. The mean donor BMI was 29, ranging from 23 to 36. The donation type was 20% donation after brain death (DBD) and 80% donation after cardiac death (DCD).
Recruitment	Human livers were procured by the organ procurement organizations (OPO) New England Donor Services (NEDS, Waltham, MA, USA) and LiveOnNY (New York, NY, USA). Informed consent was obtained by the OPO. After the livers were rejected for transplantation, they were transported to our lab under conventional hypothermic preservation (HP) conditions in University of Wisconsin Solution (UW). We excluded livers based on the following criteria: warm ischemic time >60 min, cold ischemic time >18 hours, >20% macro steatosis, donor history of liver fibrosis and any grade of liver laceration.
Ethics oversight	This study was approved by Massachusetts General Hospital (Partners IRB as an exempt protocol), New England Donor Services and LiveOn New York

Note that full information on the approval of the study protocol must also be provided in the manuscript.